Mid-infrared graphene detectors with antenna enhanced light absorption and photo-carrier collection

Yu Yao[1], Raji Shankar[1], Patrick Rauter[1], Yi Song[2], Jing Kong[2], Marko Loncar[1], and Federico Capasso[1,*]

[1] *School of Engineering and Applied Sciences, Harvard University, Cambridge, Massachusetts, 02138, USA*
[2] *Department of Electrical Engineering and Computer Science, Massachusetts Institute of Technology, Cambridge, 02139, USA*
yuyao@seas.harvard.edu

Abstract: We demonstrated antenna-assisted mid-infrared graphene detectors at room temperature with more than 200 times enhancement of responsivity (0.4 V/W at λ_0=4.45 μm) compared to devices without antennas (<2 mV/W).

1. Introduction

Graphene is an attractive material for optical detection due to its broad absorption spectrum and ultrafast response time. However, high-speed graphene detectors so far are still limited by low responsivity due to the weak optical absorption (only 2.3% in the monolayer graphene sheet) and short photocarrier lifetime (< 1 ps) [1]. Here we show that metallic nanoantenna structures can be designed to simultaneously improve both light absorption and photo-carrier collection in graphene detectors. The coupled antennas concentrate free space light into the nano-scale deep-subwavelength antenna gaps, where the graphene light interaction is greatly enhanced as a result of the ultra-high electric field intensity inside the gap. Meanwhile, the metallic antennas are designed also as electrodes to collect the generated photo-carriers very efficiently. We have demonstrated room temperature mid-infrared (mid-IR) antenna-assisted graphene detectors with more than 200 times enhancement of responsivity (0.4 V/W at λ_0=4.45 μm) compared to devices without antennas (<2 mV/W).

2. Design of antenna-assisted graphene detectors

Figure 1 (a) shows the top view of an end-to-end coupled linear antenna array on a graphene sheet and the electrical field intensity ($|E|^2/|E_0|^2$) enhancement distribution obtained by the finite difference time domain (FDTD) simulation. Light incident from free space is tightly concentrated into the near-field in the antenna gaps (gap size ~100 nm), which can greatly enhance the light-graphene interaction [2] and thus increase light absorption in graphene. The simulated current density distribution in a portion of the graphene-antenna structure (indicated by the dashed line on the top view) is shown in Fig. 1 (b). The current density distribution clearly shows that the current flows from one antenna to the graphene in the gap and then to the next antenna, as indicated by the dash-dotted arrows on the cross-section view. Thus the antenna rods also act like nano-electrodes, which can effectively collect photo-carriers generated in the nanogap between them since the maximum travelling distance for the photo-carriers generated in the gap to reach the antenna electrodes is the gap size (<100 nm in our designs). In this nano-detector, the regions with high carrier collection efficiency automatically overlap with the region where the light is focused and the majority of photo-carriers are generated. Therefore, the light absorption and photocarrier collection efficiency can be enhanced simultaneously. In our experiment, we designed the end-to-end coupled antenna structures (antenna length 900 nm, gap size 60 nm) in a 2D array to increase the light collection cross-section, as shown in Fig. 2 (c). During the device fabrication, a monolayer graphene grown via Chemical Vapor Deposition (CVD)) was first transferred onto a 30 nm dry thermal oxide layer on a highly doped silicon substrate. Then the antenna array was fabricated on the graphene sheet by electron beam lithography (EBL), electron beam evaporation of 10 nm Pd and 30 nm Au, and a lift-off process.

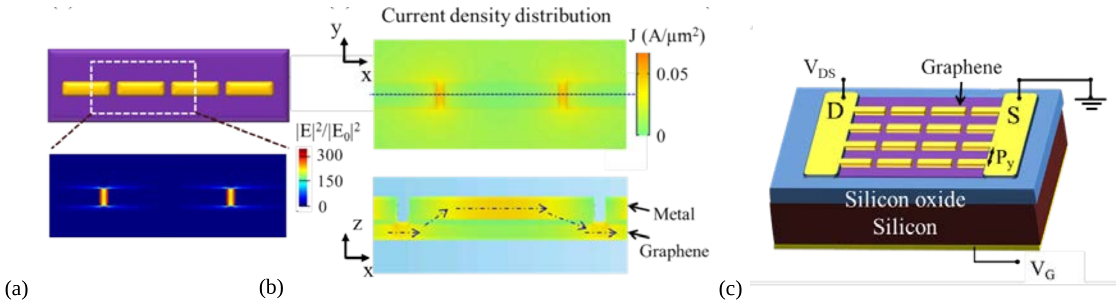

Figure 1 (a)Top view of the end-to-end coupled antennas on graphene (top) and the electric field intensity enhancement distribution on the surface of the graphene sheet (bottom). (b) Top view of the current density distribution on the surface of the graphene sheet (top) and cross-section view of the current density distribution in the middle plane of the antenna (indicated by the dashed line on the top view). The dash-dotted arrows indicate the path of the current flow. (c) A 3D schematic of the antenna-assisted graphene photodetector on a silicon substrate.

3. Detector performance characterization

The wavelength dependent responsivity of the antenna-assisted graphene detector is measured with a wavelength tunable QC laser (wavelength range: 4.3 µm to 4.7 µm). Due to the resonant nature of the plasmonic antennas, the responsivity (photo-voltage divided by the total incident power on the sample) exhibits strong wavelength dependence, as shown in Fig. 2 (a) for a device with the same structure design as that in Fig.1 (c). The responsivity reaches its maximum around 4.45 µm, which is very close to the peak wavelength (4.46 µm) of the electric field enhancement in the antenna gap calculated with FDTD simulation, also shown in Fig. 2 (a). As the bias current becomes larger, the detector responsivity increases monotonically and reaches its maximum ($R_V \approx 0.4$ V/W) at $I_{DS} \approx 4$ mA, as shown in Fig. 2 (b). Further increasing the bias leads to reduced responsivity, probably because the electric field in the graphene channel (>2 MV/m) reaches its breakdown field. A comparison between the photo-response of the graphene detectors with and without antennas is shown in Fig. 2 (c). With antenna-enhanced photo-carrier generation and collection, the photo-voltage is increased by more than 200 times compared to that of the reference sample at the same laser power. According to the FDTD simulations, the absorption at the antenna resonance wavelength is enhanced by about 4~5 times (from ~2.3% to ~10%, see more details in supplementary information III) compared with a pure monolayer graphene sheet. We attribute the additional 40~50 times improvement to the much more efficient carrier collection via metallic antennas. Moreover, the-antenna assisted graphene detector shows a linear photo-response as the incident laser power increases up to 16 mW, indicating that the absorption is not saturated despite the strong field enhancement in the antenna gaps.

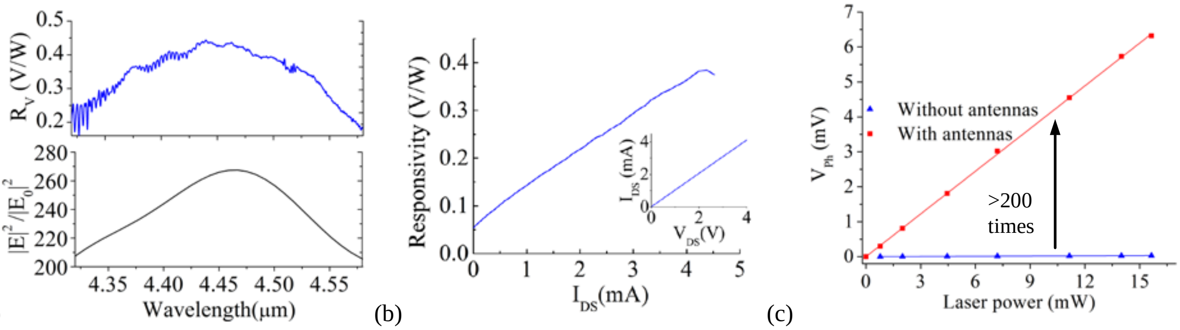

(a) (b) (c)

Fig. 2. (a) Measured wavelength dependent photo-response of the antenna-assisted graphene detector (top) and electric field intensity enhancement in the center of the nano-gap between the plasmonic antennas obtained with FDTD simulation (bottom). The narrow dips on the photo-response curve are due to absorption lines of gas molecules in the air or on the sample (mainly CO2). (b) Measured responsivity of the antenna-assisted graphene detector as a function of the biased current IDS at VGS=4 V. The inset shows the VDS-IDS plot of the same detector when the laser is off. (c) Measured photovoltage response of the graphene detectors with and without antennas as a function of incident laser power.

4. Discussion and conclusion

We have demonstrated the use of metallic optical antennas to simultaneously enhance the optical absorption and photo-carrier collection efficiency in graphene detectors and achieved room temperature mid-IR antenna-assisted graphene detectors with more than 200 times enhancement of responsivity compared to reference devices without antennas. By shrinking the detector element to deep subwavelength size, it is a promising solution to achieve high speed, ultra-compact detectors with bandwidth up to THz range. This design concept can also be applied to the graphene detectors in other wavelength ranges, such as near IR and visible wavelength, and other thin film detectors.

5. Acknowledgment

The work is supported by IARPA and AFOSR. Device fabrication was performed at the Center for Nanoscale Systems, supported by NSF.

References

[1] A. Urich, K. Unterrainer, and T. Mueller, "Intrinsic Response Time of Graphene Photodetectors," *Nano Letters*, vol. 11, pp. 2804-2808, Jul 2011.

[2] Y. Yao, M. A. Kats, P. Genevet, N. F. Yu, Y. Song, J. Kong, and F. Capasso, "Broad Electrical Tuning of Graphene-Loaded Plasmonic Antennas," *Nano Letters*, vol. 13, pp. 1257-1264, Mar 2013.